International Journal of Mechanical Sciences 74 (2013) 83–90

Contents lists available at SciVerse ScienceDirect

International Journal of Mechanical Sciences

journal homepage: www.elsevier.com/locate/ijmecsci

Balance dielectric layer for micro electrostatic switches in the presence of capillary effect

Ebrahim Yazdanpanahi, Aminreza Noghrehabadi*, Mohammad Ghalambaz

Department of Mechanical Engineering, Shahid Chamran University of Ahvaz, Ahvaz, Iran

ARTICLE INFO

Article history:
Received 29 December 2012
Received in revised form
13 April 2013
Accepted 28 April 2013
Available online 16 May 2013

Keywords:
Micro switch
Dielectric
Capillary
Pull-in
Modified Adomian
decomposition method

ABSTRACT

In this paper, the influence of capillary force on the deflection and pull-in instability of electrostatic micro actuator beams is investigated in the presence of a dielectric layer. A distributed parameter model is used to simulate the deflection of microbeam subject to the applied forces. The obtained governing differential equation of the beam is solved using the modified Adomian decomposition method (MADM). The results of MADM are compared with the numerical results of the Runge–Kutta–Fehlberg method, and they are found to be in good agreement. It is found that the voltage parameter, the capillary parameter and the dielectric parameter are the most significant parameters which affect the pull-in instability of the micro actuator. The results show that there is a specific value of dielectric parameter in which the variation of the dimensionless capillary parameter does not affect the value of maximum deflection of the micro actuator at the onset of pull-in instability. We introduced this value of dielectric parameter as Balance Dielectric Layer (BDL) because of its unique properties. There are also specific BDL values for internal stress and bending moment of the micro actuators. The BDL values are of interest for design of micro actuators in applications in which the capillary effects appeared.

1. Introduction

Over the last few years, the study of the failure mechanisms and reliability of microelectromechanical systems (MEMS) has attracted considerable attention [1,2]. There are varieties of micro actuators utilized for positioning and motion, such as scratch drive actuators, comb drives, and torsional scanner mirrors [3–5]. A typical micro actuator is constructed using two parallel electrodes, a movable electrode and a substrate. Applying molecular or external force between two electrodes causes the movable electrode to deflect into the substrate. At a critical deflection, instability occurs and the movable electrode is pulled-in onto the substrate. This phenomenon is defined at instability points of parallel plate actuators by applied electrostatic, electrochemical or capillary forces [6–8].

The pull-in characteristics of typical beams used in micro- and nano-electromechanical systems (MEMS and NEMS) have been studied by previous researchers [9–15]. Petersen [11] was the first who proposed the pull-in voltage of an electrostatic micro-actuator in 1978. Osterberg and Senturia [12] implemented tests to determine the pull-in instability of electrostatic beam actuators as well as clamped circular diaphragms. After that, many researchers conducted theoretical or experimental studies to analyze the pull-in instability of actuators.

Many researchers have analyzed the pull-in instability of micro actuators in the vacuum [13–16]. Zhe et al. [13] discussed and analyzed the pull-in voltage of parallel rigid plate actuators. Gorthi et al. [14] studied the pull-in voltage behavior of electrostatic actuators using a beam model with a dielectric layer. They identified three possible static configurations of the microbeams, namely, floating, pinned and flat configurations. They classified all possible transitions based on a dielectric layer parameter. Rollier et al. [15] as well as Noghrehabadi et al. [17] have studied the stability conditions of parallel-plate electrostatic actuators, which are embedded in liquids. They show that the pull-in instability can be shifted beyond one-third of the gap, and it can even be suppressed by changing the dielectric layer parameter. Recently, demand for design and fabrication of MEMS has been rapidly increased in applications such as electrolyte liquids (in bio applications) or drying processes [1,6,15,17].

Lin and Zhao [18] prepared an analytical solution using a lumped model to study the effect of Casimir force on the critical pull-in gap and pull-in voltage of the nonlinear model of an electrostatic actuator. Zhang and Zhao [19] developed an analytic model to consider the simultaneous effects of axial stress, residual stress, and fringing-field of the fixed-fixed micro switches. The Casimir force is very important in nano-scale dimensions, and it decreases as the dimensions increase to micro-scale; hence the

* Corresponding author. Tel.: +98 611 3330010x5678; fax: +98 611 3336642.
E-mail addresses: ebrahim8878@gmail.com (E. Yazdanpanahi), noghrehabadi@scu.ac.ir (A. Noghrehabadi), m.ghalambaz@gmail.com (M. Ghalambaz).

0020-7403/$ - see front matter © 2013 Elsevier Ltd. All rights reserved.
http://dx.doi.org/10.1016/j.ijmecsci.2013.04.014

effect of Casimir force is neglected in the analysis of micro actuators.

The capillary force usually is induced by trapping liquid (usually water) between parallel plates of beam actuators. This force, which is being in surface of micro-machined structures by wet etch of sacrificial layers, can create pull-in effect and can be the instability reason of micro-actuators. Mastrangelo and Hsu [6] were the first who analyzed the capillary force underneath a thin micromechanical structure and examined the deflection, mechanical stability and adhesion of that device. Guo et al. [7] studied static instabilities of torsion MEMS/NEMS actuators caused by capillary effects. Ouakad and Younis [8] modeled and analyzed the static behavior and collapse instabilities of doubly clamped micro beams subjected to capillary forces. They adopted a nonlinear model for the beams and examined the effect of mid-plane stretching on the pull-in length. The effect of capillary force on the pull-in instability of micro actuators in the presence of a dielectric layer has not been analyzed yet.

Wei and Zhao [20] studied the 'pull-off' situation between an Atomic Force Microscope (AFM) tip and a flat surface. They reported that the adhesion force not only depends on the water film thickness, relative humidity and the free energy of the water but also on the contact time. The adhesion force increases with the contact time in higher relative humidities [21]. Sun et al. [22] developed a theoretical model to calculate the capillary force between probe tips and nanoparticles under ambient conditions. It is shown that the tip shape and the radial distance of the meniscus have a great influence on the capillary force.

Because of the inherent nonlinearity of the forces acting on the MEMS actuators, the governing equations are also nonlinear. There are several numerical methods which can accurately integrate the governing boundary value differential equation [23–26]. However, near the pull-in stability, the numerical approaches significantly become unstable and may diverge before the pull-in instability occurs. The numerical approaches usually solve the governing equations in discrete subspaces of the domain of solution and for a specified set of physical or non-dimensional parameters. Therefore, for each set of physical or non-dimensional parameters a numerical integration of the governing equations is required.

Recently, analytical methods have been used to solve nonlinear governing equation of micro or nano actuators to obtain a solution for pull-in instability of these actuators. Zhang and Zhao [26] have analyzed pull-in stability of micro actuators subject to electrostatic forces. They have approximated the non-linear terms of the governing equations by the Taylor series expansion. Noghrehabadi et al. [27] have utilized a monotone positive solution approach based on Green's functions to study deflection of nanotube cantilevers.

The Adomian decomposition method is an analytical method proposed by Adomian for a wide class of dynamical systems without linearization, or weak nonlinearity assumptions [28]. After that, Wazwaz [29] proposed a powerful modification of the Adomian decomposition method that will accelerate the rapid convergence of the series solution. The effectiveness of the modified Adomian decomposition method has been demonstrated in many recent researches [30].

The Adomian decomposition method has been utilized to obtain pull-in deflection of electrostatic nano-actuators by Soroush et al. [31], Koochi et al. [32] and Noghrehabadi et al. [33] for cantilever beam actuators. Noghrehabadi et al. [33] have found that the results of the Adomian decomposition method are in good agreement with numerical results; however, the accuracy of the Adomian decomposition method in comparison with numerical results is comparatively low (about 10% error). Hence, they employed the Pade approximations to improve the accuracy of the solution near the pull-in instability. Koochi et al. [34] as well as Kuang and Chen [30] have employed the Modified Adomian Decomposition Method (MADM) proposed by Wazwaz [35] to study the pull-in behavior of parallel actuators. Because of rapid convergence of MADM, they [30,34] have found excellent agreement between the results of MADM and numerical results.

The objective of the present paper is to study the effect of capillary force on the pull-in instability of micro actuators in the presence of a dielectric layer. The micro actuator is modeled as a doubly clamped beam, which is subjected to the electrical and capillary forces. The distributed parameter model of the beam in its non-dimensional form depends on the non-dimensional dielectric parameter, electrical parameter, fringing field parameter and capillary parameter. The MADM is utilized to obtain an analytic solution for the nonlinear differential equation of the micro actuator beam. The dependency of the pull-in instability on the non-dimensional parameters is analytically investigated. To the best of the authors' knowledge, the results of the present paper are new, and they have not been published before.

2. Mathematical model

Fig. 1 shows a doubly clamped microbeam with a layer of dielectric on the substrate. A droplet of liquid is trapped between the top electrode and dielectric layer, which induces the capillary force. V is the external voltage difference between the top electrode and the substrate. t_d is the thickness of the dielectric layer, and L is the length of the top electrode. The rectangular cross-section of the top electrode is assumed to be uniform with thickness t and width w. The gap between the dielectric layer and top electrode is h, which is kept constant; however, the dielectric thickness can be changed.

In the present study, the static deflection of the microbeam is considered for the constitutive material of microbeam. The effective beam material (E_{eff}) for narrow beams ($w<5t$) becomes E and for wide beams ($w>5t$) becomes the plate modulus $E/(1-\nu^2)$, in which ν is the Poisson ratio [36]. The finite kinematic effect is negligible when $L>10h$ [37,38]; as most of the switches have comparatively long length, the finite kinematic effect is neglected. The capillary effects usually appear in the case of wide beams, and especially in the process of drying. The capillary force is time dependent [21]; however, in static cases the time dependent effects are neglected. It is assumed that the capillary force always acts on the entire beam. This is a realistic assumption because the wide micro actuator plates have open edges, and thus, simultaneous with the deflection of the beam, the trapped droplet can leak to the sides of the actuator [15]. Therefore, after deflection of the beam, the space between electrodes is maintained filled with the liquid. Considering the microbeam and the ground plane as two parallel rigid plates; the capillary force applied on the microbeam makes an angle θ with the unit vector that is normal

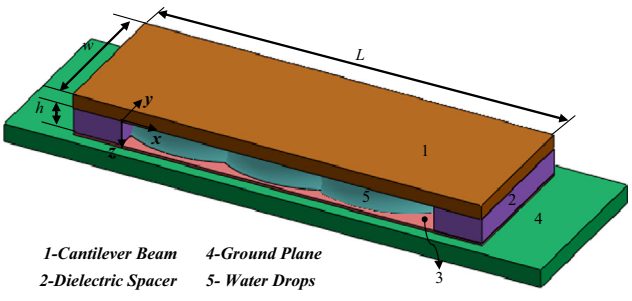

Fig. 1. Schematic representation of distributed model of fixed–fixed microbeam with a dielectric layer.

to the surface of the liquid. This force is expressed as $2\gamma_{ls}\cos(\theta_c)A_c/r$, where γ_{ls} is the surface tension of the liquid, the contact angle θ_c is the liquid–solid interfacial tension, A_c is the area of contact between the liquid and the microbeam, and r is the distance between the microbeam and the ground plane [6]. Thus, by accounting for the change in r as $h-Y$ and following the work of Legtenberg et al. [38], the capillary force per unit length of the doubly clamped microbeam is written as [6]

$$f_{cap}=\frac{2\gamma_{ls}w\cos\theta}{(h-Y)}, \tag{1}$$

where Y is the deflection of the microbeam, γ_{ls} is the surface tension of liquid and θ is the contact angle between the liquid and the beam. The water drops between the beam and the substrate may not remain rectangular. However, for the wide micro actuators, the effect of the droplets curvature on the electrical force is neglected. The fringing field effect mostly is the interaction between the electrical fields on edges of the beam; it takes place outside the micro switch and in the vacuum. Hence, the effects of the dielectric layer and liquid beneath the beam on the electrical force are taken into account. However, the effect of the dielectric layer as well as liquid droplets beneath the beam on the fringing filed effect may be neglected. Considering the first order fringing field correction in the absence of liquid and dielectric, the electrostatic force per unit length of the doubly clamped microbeam is defined as [39,40]

$$f_{elec}=\frac{\varepsilon_0\varepsilon wV^2}{2(t_d\varepsilon/\varepsilon_d+h-Y)^2}+\frac{\varepsilon_0V^2}{2}\frac{0.65}{(h+t_d-Y)}, \tag{2}$$

where $\varepsilon_0=8.854\times10^{-12}$ c^2/Nm^2 is the permittivity of the vacuum, and ε is the relative permittivity of the medium. t_d and ε_d are the thickness and relative permittivity of the insulating layer, respectively. V is the external voltage difference between the substrate and the beam.

It is noted that when the maximum deflection is less than the thickness, small deflection can be considered valid, and the stretching effects can be neglected [19]. Considering small deflections of the microbeam and applying the virtual work principle, the appropriate approximation of the beam deflection in the absence of the non-conservative forces can be obtained as fallows [31]:

$$\delta W=\delta E_{elast}-\delta W_{elec}-\delta W_{cap}=\int_0^L\left(E_{eff}I\frac{d^2Y}{dX^2}\delta\frac{d^2Y}{dX^2}-f_{elec}\delta Y-f_{cap}\delta Y\right)dX \tag{3}$$

Integrating Eq. (3) yields

$$\delta W=E_{eff}I\frac{d^2Y}{dX^2}\delta\frac{dY}{dX}\Big|_0^L-E_{eff}I\frac{d^3Y}{dX^3}\,\delta y\Big|_0^L+\int_0^L\left(E_{eff}I\frac{d^4Y}{dX^4}-f_{elec}-f_{cap}\right)\delta Y\,dX \tag{4}$$

The deflection of the microbeam is evaluated by the following boundary-value differential equation

$$E_{eff}I\frac{d^4Y}{dX^4}=f_{elec}+f_{cap}, \tag{5-a}$$

and the geometrical boundary conditions at the fixed ends as

$$Y(0)=Y'(0)=0,\quad Y(L)=Y'(L)=0 \tag{5-b}$$

where X is the position along the beam measured from the one end, and I is the moment of inertia of the beam cross section [36]. By substituting Eqs. (1) and (2) into Eq. (5-a) and introducing the non-dimensional variables as

$$\beta=\frac{\varepsilon_0\varepsilon wL^4V^2}{2h^3E_{eff}I},\quad \gamma_{fr}=0.65\frac{h}{w}\frac{\beta}{\varepsilon},\quad K=\frac{t_d}{\varepsilon_r h},$$
$$\gamma_{ca}=\frac{2\gamma_{ls}\,w\,L^4\cos\theta}{EIh^2},\quad x=X/L,\quad g=1-Y/h, \tag{6}$$

the governing equation can be written in the following non-dimensional form:

$$\frac{d^4g}{dx^4}=-\frac{\beta}{(K+g(x))^2}-\frac{\gamma_{fr}}{K\varepsilon_r+g(x)}-\frac{\gamma_{ca}}{g(x)}, \tag{7-a}$$

where g is the non-dimensional deflection of the beam and x is the non-dimensional parameter along the beam. β, γ_{fr}, K and γ_{ca} are the applied voltage parameter, fringing field parameter, dielectric-layer parameter and capillary parameter, respectively. ε_r is the ratio of the relative dielectric permeability to the relative permeability of liquid ($\varepsilon_r=\varepsilon_d/\varepsilon$). In the following text, the value of ε_r is assumed to be 8.0/80.1, where 8.0 is the equivalent permeability of insulating layer (SixNy [15]), and 80.1 is the relative permeability of liquid (water) [15]. The non-dimensional boundary conditions at the fixed ends are

$$g(0)=g'(0)=0, \tag{7-b}$$

$$g(1)=g'(1)=0, \tag{7-c}$$

where prime denotes differentiation with respect to x.

3. Analytic solution

3.1. Modified Adomian decomposition method

The Adomian polynomials are very powerful in solving nonlinear differential equations [35,41,42]. Different modifications of the Adomian decomposition method have been proposed by recent researchers [43–47]. The modified Adomian decomposition method was established as a very effective, simple and convenient method by Wazwaz in 1999 to solve nonlinear initial and boundary value problems [29]. Here, MADM has been implemented to solve the governing equation of the micro beam, Eq. (7-a), subject to the boundary conditions of Eqs. (7-b) and (7-c).

Consider the boundary value problem of the forth order differential equation in the form

$$d^4g/dx^4=N(g(x)), \tag{8-a}$$

subject to the following boundary conditions

$$g(0)=1,\quad g'(0)=0, \tag{8-b}$$

$$g(1)=1,\quad g'(1)=0, \tag{8-c}$$

where $N(g(x))$ can be linear or nonlinear functions. $g(x)$ can be written as

$$g(x)=\sum_{n=0}^{\infty}g_n(x), \tag{9}$$

Here, $N(g(x))$ is the right hand side of Eq. (7-a) and can be approximated by a series of Adomian polynomials [48].

$$N(g(x))=\sum_{n=0}^{\infty}N_n(x). \tag{10}$$

According to specific algorithm established by Adomian, the polynomials N_n are the so-called Adomian polynomials which can be generated for various kinds of nonlinearity. Eq. (8-a) can be rewritten in the operator form by substituting Eq. (9) into Eq. (8-a)

as follows:

$$L^{(4)}(g(x)) = \sum_{n=0}^{\infty} N_n(x), \tag{11}$$

where $L^{(4)}$ is the differential operator given as

$$L^{(4)} = \frac{d^{(4)}}{dx^{(4)}}, \tag{12}$$

and the inverse operator $L^{-(4)}$ is defined as a forth-fold integral operator [28],

$$L^{-(4)} = \int_0^x \int_0^x \int_0^x \int_0^x (.)\, dxdxdxdx. \tag{13}$$

By considering the governing differential equation of microbeam (Eq. (7-a)) and employing introduced operator (Eq. (13)) to Eq. (8-a), the dependent variable ($g(x)$) can be written as [29],

$$g(x) = \sum_{n=0}^{\infty} g_n(x) = d_0 + d_1 x + \tfrac{1}{2} d_2 x^2 + \tfrac{1}{6} d_3 x^3 + L^{-(4)}\left[\sum_{n=0}^{\infty} N_n(x)\right], \tag{14-a}$$

where the constants of d_0 to d_3 are:

$$d_0 = g(0), \quad d_1 = g'(0), \tag{14-b}$$

$$d_2 = g''(0), \quad d_3 = g'''(0). \tag{14-c}$$

The constants of d_2 and d_3 are evaluated later by the solution of the algebraic equations which comes from the boundary conditions at $x=1$. According to the modified Adomian decomposition method [29], the recursive relations of Eq. (14-a) are demonstrated as follows:

$$g_0(x) = d_0, \tag{15-a}$$

$$g_1(x) = d_1 x + \tfrac{1}{2} d_2 x^2 + \tfrac{1}{6} d_3 x^3 + L^{-(4)}[N_0(x)], \tag{15-b}$$

$$g_k(x) = L^{-(4)}[N_{k-1}(x)]. \tag{15-c}$$

The Adomian polynomial N_n can be derived by the following convenient equations [29,49]:

$$N_n = \sum_{v=1}^{n} C(v,n) H_v(g_0), \quad (n>0), \tag{16-a}$$

$$C(v,n) = \sum_{p_i} \prod_{i=1}^{v} \frac{g_{pi}^{ki}}{k!}, \quad \left(\sum_{i=1}^{v} k_i p_i = n,\ 0 \le i \le n,\ 1 \le p_i \le n-v+1\right), \tag{16-b}$$

$$H_v(g_0) = d^v / dg_0{}^v [N(g_0)], \tag{16-c}$$

where k_i is the number of repetitions in g_{pi} and the values of p_i are selected from the above range by a combination without repetition. Here, the dependent variable, $g(x)$, can be represented by employing the Adomian decomposition method,

$$g(x) = \sum_{n=0}^{\infty} g_n(x) = d_0 + d_1 x + \tfrac{1}{2} d_2 x^2 + \tfrac{1}{6} d_3 x^3 - \beta L^{-(4)}\left[\sum_{n=0}^{\infty} A_n(x)\right] - \gamma_{fr} L^{-(4)}\left[\sum_{n=0}^{\infty} B_n(x)\right] - \gamma_{ca} L^{-(4)}\left[\sum_{n=0}^{\infty} C_n(x)\right]. \tag{17}$$

It is convenient to obtain the Adomian polynomials as

$$A_0 = \frac{1}{(K+g_0)^2}, \quad B_0 = \frac{1}{(K\varepsilon_r + g_0)}, \quad C_0 = \frac{1}{g_0}, \tag{18-a}$$

$$A_1 = g_1 H_1(g_0) = -\frac{2g_1}{(K+g_0)^3}, \quad B_1 = -\frac{g_1}{(K\varepsilon_r + g_0)^2}, \quad C_1 = -\frac{g_1}{g_0{}^2}, \tag{18-b}$$

$$A_2 = g_2 H_1(g_0) + \tfrac{g_1^2}{2!} H_2(g_0) = -\tfrac{2g_2}{(K+g_0)^3} + \tfrac{3g_1{}^2}{(K+g_0)^4},$$
$$B_2 = -\frac{g_2}{(K\varepsilon_r + g_0)^2} + \frac{g_1{}^2}{(K\varepsilon_r + g_0)^3}, \quad C_2 = -\frac{g_2}{g_0{}^2} + \frac{g_1{}^2}{g_0{}^3}. \tag{18-c}$$

Let $g_0(x) = d_0$, then,

$$g_1(x) = d_1 x + (1/2) d_2 x^2 + (1/6) d_3 x^3 - \left(\frac{\beta}{24(d_0+K)^2} - \frac{\gamma_{fr}}{24(d_0+K\varepsilon_r)} - \frac{\gamma_{ca}}{24 d_0}\right) x^4, \tag{19-a}$$

$$g_2(x) = \left(\frac{\beta d_1}{60(d_0+K)^3} + \frac{\gamma_{fr} d_1}{120(d_0+K\varepsilon_r)^2} + \frac{\gamma_{ca} d_1}{120 d_0{}^2}\right) x^5 + \left(\frac{\gamma_{fr} d_2}{720(d_0+K\varepsilon_r)^2} + \frac{\gamma_{ca} d_2}{720 d_0{}^2} + \frac{\beta d_2}{360(d_0+K)^3}\right) x^6 + \left(\frac{\gamma_{fr} d_3}{5040(d_0+K\varepsilon_r)^2} + \frac{\gamma_{ca} d_3}{5040 d_0{}^2} + \frac{\beta d_3}{2520(d_0+K)^3}\right) x^7 - \left(\begin{array}{l} \frac{\gamma_{ca}\cdot\beta}{40320 d_0{}^2 (d_0+K)^2} + \frac{\gamma_{fr}\cdot\beta}{40320(d_0+K\varepsilon_r)^2 (d_0+K)^2} \\ + \frac{\gamma_{fr}{}^2}{40320(d_0+K\varepsilon_r)^3} + \frac{\gamma_{ca}{}^2}{40320 d_0{}^3} + \frac{\gamma_{fr}\cdot\gamma_{ca}}{40320(d_0+K\varepsilon_r)^2 d_0} \\ + \frac{\gamma_{fr}\cdot\gamma_{ca}}{40320(d_0+K\varepsilon_r) d_0{}^2} + \frac{\beta^2}{20160(d_0+K)^5} \\ + \frac{\beta\cdot\gamma_{fr}}{20160(d_0+K\varepsilon_r)(d_0+K)^3} + \frac{\beta\cdot\gamma_{ca}}{20160 d_0 (d_0+K)^3} \end{array}\right) x^8 \tag{19-b}$$

Therefore, by applying the boundary conditions at $x=0$, the constants d_0 and d_1 are concluded as 1 and 0, respectively. Regarding the unknown coefficients of d_2 and d_3, the polynomial solution of Eq. (8-a) is obtained by the sum of three terms, which can be summarized as

$$g(x) = g_0(x) + g_1(x) + g_2(x) + ..., \tag{20-a}$$

The undetermined coefficients, d_2 and d_3, will be calculated later by using the boundary conditions at the $x=1$ (i.e., Eq. (7-c)) for any given set of non-dimensional parameters.

Because of the symmetry of the micro beam, the maximum deflection occurred at $x=1/2$, which is denoted by u_{max}, where u is considered as Y/h. In order to study the instability of micro-actuators, the maximum deflection at the onset of pull-in instability can be obtained from Eq. (20-b) by setting $du_{max}/d\zeta \to \infty$. Here, ζ is the parameter of interest, which could be each of the non-dimensional parameters. No solution exists for $u(x)$ by increasing the non dimensional parameters beyond the pull-in instability. Hence, all the parameters and variables at this point are shown by PI subscript.

$$g(x) = 1 + (1/2)d_2x^2 + (1/6)d_3x^3 - \left(\frac{\beta}{24(1+K)^2} - \frac{\gamma_{fr}}{24(1+K\varepsilon_r)} - \frac{\gamma_{ca}}{24}\right)x^4 + \left(\frac{\gamma_{fr}d_2}{720(1+K\varepsilon_r)^2} + \frac{\gamma_{ca}d_2}{720} + \frac{\beta d_2}{360(1+K)^3}\right)x^6$$
$$+ \left(\frac{\gamma_{fr}d_3}{5040(1+K\varepsilon_r)^2} + \frac{\gamma_{ca}d_3}{5040} + \frac{\beta d_3}{2520(1+K)^3}\right)x^7 - \left(\begin{array}{l} \frac{\beta.\gamma_{ca}}{40320(1+K)^2} + \frac{\beta.\gamma_{fr}}{40320(1+K)^2(1+K\varepsilon_r)^2} \\ + \frac{\gamma_{fr}{}^2}{40320(1+K\varepsilon_r)^3} + \frac{\gamma_{ca}{}^2}{40320} + \frac{\gamma_{fr}.\gamma_{ca}}{40320(1+K\varepsilon_r)^2} \\ + \frac{\gamma_{fr}.\gamma_{ca}}{40320(1+K\varepsilon_r)} + \frac{\beta^2}{20160(1+K)^5} \\ + \frac{\beta.\gamma_{fr}}{20160(1+K)^3(1+K\varepsilon_r)} + \frac{\beta.\gamma_{ca}}{20160(1+K)^3} \end{array}\right)x^8, \quad (20-\text{b})$$

3.2. Comparison between MADM and previous results

Eq. (7-a) subjected to the boundary conditions of Eqs. (7-b) and (7-c) is numerically solved using the Runge–Kutta–Fehlberg method [50] with a relative tolerance of 10^{-7}. Neglecting the dielectric layer and capillary effects, the model of the present study reduces to the work of Osterberg and Senturia [12] as well as Kuang and Chen [30]. Here, two microbeams with $L=250$ and 350 μm, $w=50$ μm, $h=1$ μm, $t=3$ μm, $E=169$ GPa and $\nu=0.06$ subject to electrostatic force [12,30] are considered. Table 1 shows a comparison between the pull-in voltage obtained by previous researchers and the results of MADM as well as the numerical method. As seen, the relative error between the results of MADM and the MEMCAD software [12] is less than 2%.

In order to verify the accuracy and convergence of the analytical method in the presence of dielectric layer and capillary effects, the pull-in deflection of a typical micro actuator is evaluated using the MADM and compared with the results of the numerical method. The analytical results of MADM are obtained for five to nine terms of MADM when $K=0.5$, $\gamma_{ca}=30$, $\beta=130$ and $\varepsilon_r=0.1$. In this case, the comparison between the analytical results and numerical results is shown in Table 2. In this table, $u_{max,Num}$ and $u_{max,MADM}$ are the maximum beam deflection using numerical method and analytical method respectively. The results of Table 2 show that the analytical solution converges to the numerical solution as the number of the series terms increases, and a higher accuracy can be achieved by evaluating more terms of the modified Adomian series. Comparison between the analytical results and numerical results in Table 2 illustrates that eight terms of the modified Adomian series ($O(x^{-29})$) have relative error less than 0.03%, which shows good agreement between analytical and numerical solutions. Hence, eight terms of the modified Adomian series are selected in the following calculations for convenience.

4. Results and discussion

Based on Eq. (6), the fringing field parameter (γ_{fr}) is a function of h/w and β. However, considering a practical nanobeam with $L=350$ μm, $w=50$ μm, $h=1$ μm, $t=3$ μm, which has been previously analyzed by Osterberg and Senturia [12], demonstrates that h/w is constant for a specified microbeam, and hence, the fringing field parameter can be assumed only as a function of β. The voltage parameter (β) can be changed by changing the voltage value (V). Therefore, changing the voltage value can also change the voltage parameter (β) and fringing parameter simultaneously. By this assumption, the pull-in stability of the microbeam is a

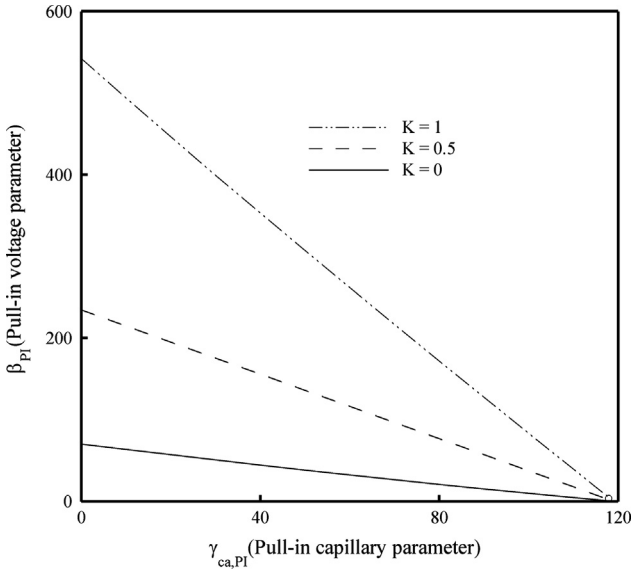

Fig. 2. Effect of dielectric layer parameter on the pull-in capillary parameter.

Table 1
Comparison between pull-in voltage obtained by MADM and previous studies for a microbeam affected just by electrostatic force with $h=1$ μm, $w=50$ μm, and $t=3$ μm.

Beam length (μm)	Pull-in voltage (V_{PI})					$\left\|\frac{V_{PI,\ MEMCAD}-V_{PI,\ MAD}}{V_{PI,\ MEMCAD}}\right\| \times 100$
	ADM [15]	(2-D) [6]	MEMCAD [6]	Numerical (present)	MAD method (present)	
250	39.6	39.5	40.1	39.1	39.3	2
350	20.2	20.2	20.3	20.0	20.1	1

Table 2
Variation of the maximum deflection of a microbeam (u_{max}) evaluated with selected terms of MADM for $K=0.5$, $\gamma_{ca}=30$ and for $\beta=130$.

Tip deflection	5 Terms (x^{16})	6 Terms (x^{20})	7 Terms (x^{24})	8 Terms (x^{28})	9 Terms (x^{32})
MADM	0.326911	0.329634	0.330474	0.330731	0.30810
Numerical			0.330846		
Error% $= \left\|\frac{u_{max,MADM}-u_{max,Num}}{u_{max,Num}}\right\| \times 100$	1.19	0.37	0.11	0.03	0.01

function of the three remaining non-dimensional parameters of dielectric layer (K), voltage (β) and capillary (γ_{ca}).

By solving Eq. (7) for a range of capillary parameter and selected values of the dielectric parameter, the pull-in voltage β_{PI} is obtained. Fig. 2 shows the effect of the capillary parameter on the voltage parameter at the onset of pull-in instability for selected values of dielectric layer parameter. This figure reveals that an increase of the capillary parameter would decrease the pull-in voltage parameter. As seen, in the case of $K=0.5$, the required values of β_{PI} are two-fold of $\gamma_{ca,PI}$.

This observation is in good agreement with physics of the microbeams because the presence of an external force reduces the required voltage for pull-in instability. From a physical point of view, it is worth noticing that the presence of capillary force or dielectric layer, appearing in Eq. (7-a), have different physical insights. The capillary parameter indicates the presence of an external force, but the dielectric layer parameter indicates the resistance in electrical force of the microbeam.

Fig. 3 depicts the effect of the capillary parameter on the pull-in deflection of the microbeam for selected values of dielectric layer parameter. This figure reveals that there are three distinct trends of behavior for the variation of beam deflection with the increase of capillary parameter. For the dielectric layer parameter which its magnitude is comparatively less than 0.5 ($K=0$), as the capillary parameter increases the pull-in deflection increases. In contrast, for the values of the dielectric layer parameter comparatively higher than 0.5 ($K=1.0$), the influence of the capillary parameter on the pull-in deflection is inverted. In this case, as the capillary parameter increases the maximum deflection (beam deflection) at the onset of pull-in instability decreases. This observed difference between two curves (i.e., $K=0$ and $K=1.0$) is because of the fact that the presence of a dielectric layer increases the pull-in deflection induced by electrical forces. For a dielectric parameter of $K\approx0.5$, the variation of the capillary parameter does not show any significant effect on the pull-in deflection. Thus, for the dielectric parameter of $K\approx0.5$, the beam deflection is independent of the capillary effects. This interesting value of dielectric parameter is introduced as the Balance Dielectric Layer (BDL) which is denoted by K^*. Here, in order to analyze the balance dielectric layer in Fig. 3 (the straight line represent by $K=0.5$), the following two critical cases from the general model, Eq. (7-a), are studied:

$$\frac{d^4g}{dx^4} = -\frac{\beta}{(0.5+g(x))^2} - \frac{\gamma_{fr}}{(0.5\varepsilon_r + g(x))} \qquad (22-a)$$

$$\frac{d^4g}{dx^4} = -\frac{\gamma_{ca}}{g(x)} \qquad (22-b)$$

Eq. (22-a) neglects the effect of capillary parameter and assumes a microbeam with a dielectric layer which affected only by the electrostatic force when $K=0.5$. Here, for the discussion, temporary the effect of fringing field parameter can be neglected due to the presence of the large value of relative permittivity of liquid on denominator of its definition, i.e., $\gamma_{fr}=0.65(h/w)\beta/\varepsilon$ and $\varepsilon=80.1$. Therefore, in Eq. (22-a) the term $\beta/(0.5+g)^2$ is the dominant term. Eq. (22-b) neglects the electrostatic force and supposes a microbeam affected just by capillary force. By these assumptions, the deflection of beam in these critical cases is either a function of $\beta/(0.5+g)^2$ based on Eq. (22-a) or γ_{ca}/g based on Eq. (22-b).

It is trivial that the deflection of the beam is the result of forces which act on the beam. Hence, increasing the capillary effect decreases the required pull-in voltage (as seen in Fig. 2). Indeed, the appearing of capillary effect increases the effect of the capillary term in Eq. (7-a) and tends to transfer the beam deflection trend from pure electrical force (Eq. (22-a)) into pure capillary force (Eq. (22-b)). As mentioned, in the case of $K\approx0.5$, the variation of the capillary parameter does not affect the pull-in deflection of the microbeam. In order to discover the basis of this phenomenon, the magnitude of $2/(K+g)^2$ and $1/g$ for $K=0.5$ and arbitrary values of non-dimensional pull-in deflection (g) are shown in Table 3. It is worth noticing that the multiplicative value of 2.0 in the term $2/(K+g)^2$ comes from the basis of Fig. 2, which shows that the required value of pull-in voltage parameter is two-fold of the required pull-in capillary parameter. As seen, the calculated values of these functions, i.e. $2/(K+g)^2$ and $1/g$, are very close to each other. Therefore, in this case, i.e., $K=K^*$, the appearing of capillary effect, which tends to transfer the beam deflection trend from the pure electrical force to pure capillary force, transfers the beam deflection trend between two functions which are almost similar. It means that in the case of $K=K^*$ both parameters of pull-in capillary and pull-in voltage can be replaced by each other without any changing in the pull-in deflection of microbeam.

The corresponding values of non-dimensional pull-in deflections for pure electrical force with $K=K^*=0.5$ (Eq. (22-a)) and pure capillary force (Eq. (22-b)) are marked in Fig. 3. In this figure the obtained values of pull-in deflection for both of the equations, i.e., Eqs. (22-a) and (22-b), are almost 0.62. However, in a general case, the effect of the voltage force is different from the capillary force. As seen in Fig. 3 for cases of $K=0$ and $K=1.0$, at the onset of pull-in instability different values of pull-in deflection are obtained. The magnitude of non dimensional deflection for pure electrical force, with $K=0$ and $K=1$ are 0.41 and 0.8, respectively; while the pull-in deflection for the pure capillary force, Eq. (22-b), is 0.62. Therefore, by increasing the capillary effect, the non-dimensional pull-in deflection increases from 0.41 (pure electrical force) to 0.62 (pure capillary force). However, in the case of $K=1.0$ the

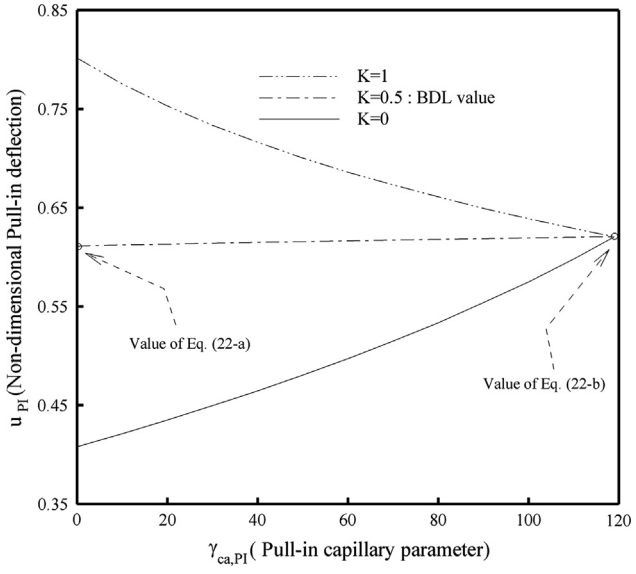

Fig. 3. Effect of capillary parameter and dielectric layer parameter on the maximum pull-in deflection of microbeam.

Table 3
Comparison for normal behavior of $1/g$ and $2/(0.5+g)^2$ functions.

g	$1/g$	$2/(0.5+g)^2$
0.3	3.33	3.13
0.4	2.5	2.47
0.5	2.0	2.0
0.6	1.67	1.65
0.7	1.43	1.39

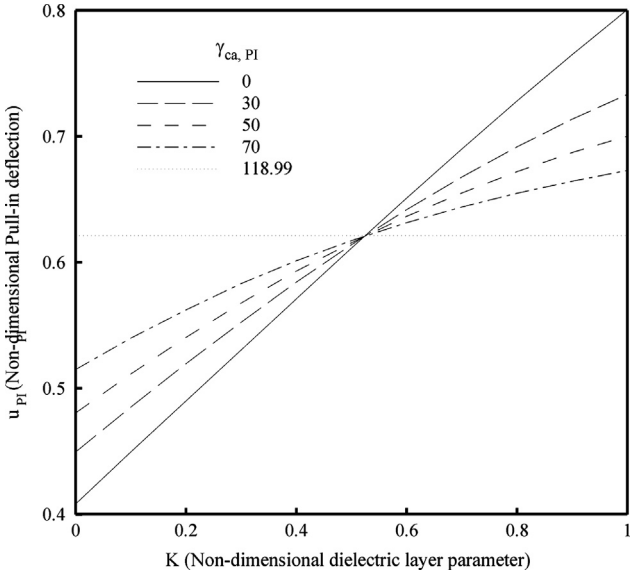

Fig. 4. Balance dielectric layer of microbeam for maximum deflection.

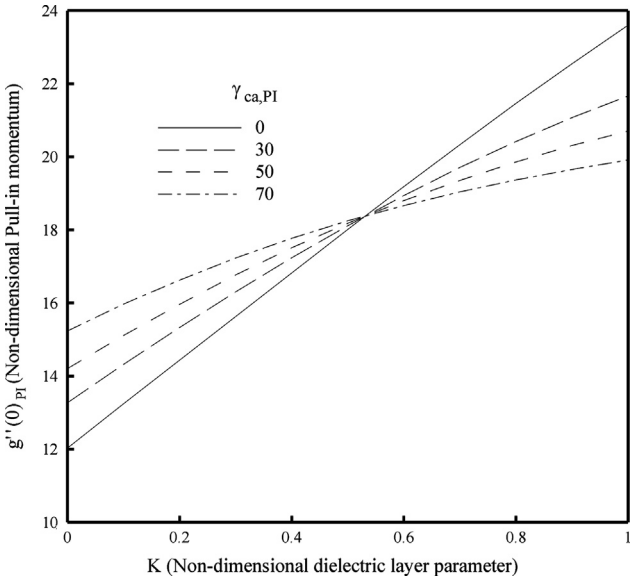

Fig. 5. Balance dielectric layer of microbeam for maximum momentum.

corresponding pull-in deflection of the electrical force (0.8) is higher than that of the capillary force (0.62). Therefore, an increase in the capillary effect decreases the pull-in deflection. As mentioned, in the case of $K=0.5$ the corresponding pull-in deflection of the pure electrical force (0.62) and pure capillary force (0.62) are equal. Hence, increasing the capillary effects transfers the pull-in deflection from 0.62 to 0.62 which is the straight (dashed point) line in Fig. 3.

Fig. 4 shows non-dimensional deflection of the microbeam for selected values of capillary parameter and a range of dielectric parameters (K between 0 and 1). A focal point can be seen for all curves plotted in this figure. This point introduces the value of balance dielectric layer for pull-in deflection of a typical microbeam. This point demonstrates that there is a distinct dielectric-layer parameter in which the variation of the dimensionless capillary parameter does not affect the values of pull-in deflection, which were introduced as the balance dielectric layer. The balance dielectric layer phenomenon occurred in this typical microbeam because the microbeam is subjected to the simultaneous effects of dielectric layer and capillary force.

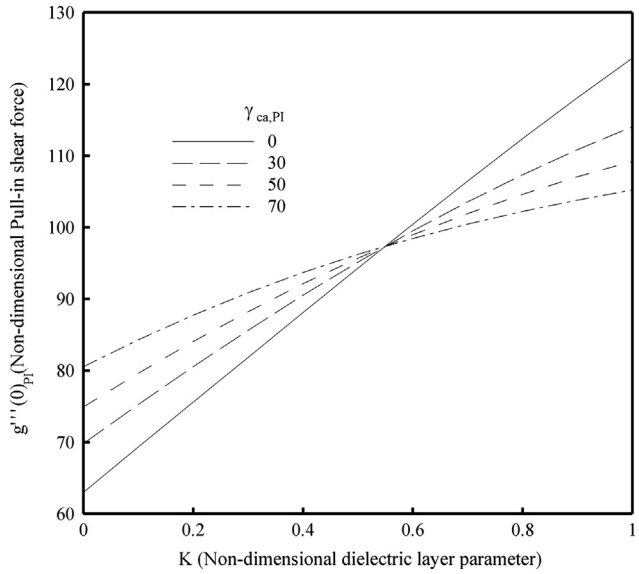

Fig. 6. Balance dielectric layer of microbeam for maximum shear force.

Table 4
Maximum deflection, shear force and bending momentum in pull-in situation of microbeam at balance dielectric layer obtained using MADM.

Fig. 4		Fig. 5		Fig. 6	
K^*	u_{PI}	K^*	$g''(0)_{PI}$	K^*	$g'''(0)_{PI}$
0.524	0.6212	0.533	18.406	0.549	97.343

Stress analysis of a micro device is important for controlling the mechanical properties of materials [51] and avoiding the failing of the device after operation [31]. As known, the maximum bending moment and shear force always occur at the boundary end points of a fixed–fixed microbeam with uniform cross-section of area [36]. The maximum value of internal stress resultants of the microbeam at the onset of pull-in instability can be defined as [31]

$$\sigma_{PI,\max} = g''_{PI}(0) \times htE_{eff}/(2L^2), \quad (23-a)$$

$$\tau_{PI,\max} = g'''_{PI}(0) \times ht^2E_{eff}/(8L^3), \quad (23-b)$$

where $\sigma_{PI,\max}$ is the maximum normal stress, and $\tau_{PI,\max}$ is the maximum shear stress at the initial cross-section of the microbeam. Figs. 5 and 6 show the effect of the dielectric parameter on the values of $g''(0)$ and $g'''(0)$, respectively. It can be observed that the values of DBL in Figs. 4–6 are not identical. Therefore, the corresponding values of K^* for the important design parameters of the microbeam, which are the pull-in deflection, shear force and bending moment, are shown in Table 4.

5. Conclusion

The pull-in instability of an electrostatic doubly clamped microbeam in the presence of a dielectric layer and capillary force is investigated. The modified Adomian decomposition method is successfully utilized to obtain the pull-in instability of microbeam. The comparison between analytical results and numerical results shows that the eight terms of the Adomian series (i.e., x^{28}) provide sufficient accuracy for most engineering designs. The results show that presence of a dielectric layer increases the pull-in deflection induced by electrical forces; however, presence of capillary effects

may increase or decrease the pull-in deflection. The variation of pull-in deflection affects the pull-in tensions (the pull-in shear force and bending moment) of the microbeam actuator. It is found that there is a specific value of dielectric parameter in which the variation of the capillary parameter does not show any significant effect on the pull-in deflection of the microbeam. This value of the dielectric parameter was introduced as the Balanced Dielectric Layer (BDL). For each of the other important design parameters, i.e., pull-in deflection, shear force and bending moment, there is a specific value of dielectric parameter (BDL) in which the variation of that design parameter is independent of the capillary effect.

The calculated values of BDL can be very useful in designing the microbeams actuators in the applications in which the presence of capillary effects are common. Designing a microbeam with dimensions and physical parameters, in which the non-dimensional dielectric parameter of the microbeam is equal to the BDL value, can eliminate the effect of capillary force on the pull-in deflection of the microbeam.

References

[1] Merlijn van Spengen W. MEMS reliability from a failure mechanisms perspective. Microelectron Reliab 2003;43:1049–60.
[2] Hsu TR. Reliability in MEMS packaging. In: Proceedings of an invited paper, 44th International Reliability Physics Symposium, San Jose, CA, 2006.
[3] Akiyama T, Shono K. Controlled stepwise motion in polysilicon microstructures. J Microelectromech Syst 1993;2(3):106–10.
[4] Akiyama T, Collard D, Fujita H. Scratch drive actuator with mechanical links for self-assembly of three dimensional MEMS. J Microelectromech Syst 1997;6(1):10–7.
[5] Honarmandi P, Zu JW, Behdinan K. Analytical study and design characteristics of scratch drive actuators. Sensors Actuators A 2010;160:116–24.
[6] Mastrangelo CH, Hsu CH. Mechanical stability and adhesion of microstructures under capillary forces: Part I: basic theory. J Microelectromech Syst 1993;2:33–43.
[7] Guo JG, Zhou LJ, Zhao YP. Instability analysis of torsional MEMS/NEMS actuators under capillary force. J Colloid Interface Sci 2009;331:458–62.
[8] Ouakad HM, Younis MI. modeling and simulations of collapse instabilities of microbeams due to capillary forces. Math Probl Eng 2009:871902 [Article ID].
[9] Boyd IV JG, Kim D. Nanoscale electrostatic actuators in liquid electrolytes. J Colloid Interface Sci 2006;301:542–8.
[10] Boyd IV JG, Lee J. Deflection and pull-in instability of nanoscale beams in liquid electrolytes. J Colloid Interface Sci 2011;356:387–94.
[11] Petersen KE. Dynamic micromechanics on silicon: techniques and devices. IEEE Trans Electron Devices 1978;ED 25:1241–50.
[12] Osterberg PM, Senturia SD. M-TEST: a test chip for MEMS material property measurement using electrostatically actuated test structures. J Microelectromech Syst 1997;6:107–18.
[13] Cheng J, Zhe J, Wu X. Analytical pull-in study on non-deformable electrostatic micro actuators. In: Technical Proceedings of the 2002 International Conference on Modeling and Simulation of Microsystem. Nanotechnology 1;298–301.
[14] Gorthi S, Mohanty A, Chatterjee A. Cantilever beam electrostatic MEMS actuators beyond pull-in. J Micromech Microeng 2006;16:1800–10.
[15] Rollier AS, Legrand B, Collard D, Buchaillot L. The stability and pull-in voltage of electrostatic parallel-plate actuators in liquid solutions. J Micromech Microeng 2006;16:794–801.
[16] Koochi A, Noghrehabadi AR, Abadyan MR. Approximating the effect of van der Waals force on the instability of electrostatic nano-cantilevers. Int J Mod Phys B 2011;25(29):3965–76.
[17] Noghrehabadi AR, Eslami M, Ghalambaz M. Influence of size effect and elastic boundary condition on the pull-in instability of nano-scale cantilever beams immersed in liquid electrolytes. Int J Nonlinear Mech 2013;52:73–84.
[18] Lin WH, Zhao YP. Casimir effect on the pull-in parameters of nanometer switches. Microsyst Technol 2005;11:80–5.
[19] Zhang LX, Zhao YP. Electromechanical model of RF MEMS switches. Microsyst Technol 2003;9:420–6.
[20] Zh. Wei, Zhao Y-P. Experimental investigation of the velocity effect on adhesion forces with an atomic force microscope. Chin Phys Lett 2004;21(4):616–9.
[21] Wei Zh, Zhao Y-P. Growth of liquid bridge in AFM. J Phys D Appl Phys 2007;40:4368–75.
[22] Sun LN, Wang LF, Rong WB. Capillary interactions between a probe tip and a nanoparticle. Chin Phys Lett 2008;25(5):1795–8.
[23] AbdelRahman ME, Younis MI, Nayfeh AH. Characterization of the mechanical behavior of an electrically actuated microbeam. J Micromech Microeng 2002;12:759–66.
[24] Ouakad HM, Younis MI. The dynamic behavior of MEMS arch resonators actuated electrically. Int J Nonlinear Mech 2010;45:704–13.
[25] Zhang Y, Zhao Y. Static study of cantilever beam stiction under electrostatic force influence. Acta Mech Solida Sin 2004;17(2):104–12.
[26] Zhang Y, Zhao YP. Numerical and analytical study on the pull-in instability of micro-structure under electrostatic loading. Sensors Actuators A 2006;127:366–80.
[27] Noghrehabadi A, Ghalambaz M, Ghanbarzadeh A. Buckling of multi wall carbon nanotube cantilevers in the vicinity of graphite sheets using monotone positive method. J Comput Appl Res Mech Eng 2012;1:89–97.
[28] Adomian GA. Review of the decomposition method in applied mathematics. J Math Anal Appl 1988;135:501–44.
[29] Wazwaz AM. A reliable modification of Adomian decomposition method. Appl Math Comput 1999;102:77–86.
[30] Kuang JH, Chen CJ. Adomian decomposition method used for solving nonlinear pull-in behavior in electrostatic micro-actuators. Math Comput Model 2005;41:1479–91.
[31] Soroush R, Koochi A, Kazemi AS, Haddadpour H, Abadyan M. Investigating the effect of Casimir and van der Waals attractions on the electrostatic pull-in instability of nano-actuators. Phys Scr 2010;82:045801.
[32] Koochi A, Kazemi AS, Noghrehabadi A, Yekrangi A, Abayan M. New approach to model the buckling and stable length of multi walled carbon nanotube probes near graphite sheets. Mater Des 2005;32:2949–55.
[33] Noghrehabadi A, Ghalambaz M, Ghanbarzadeh A. the electrostatic pull-in instability of nanocantilever actuators using the ADM-Padé technique. Comput Math Appl 2012;64:2806–15.
[34] Koochi A, Kazemi AS, Tadi Beni Y, Yekrangi A, Abayan M. Theoretical study of the effect of Casimir attraction on the pull-in behavior of beam-type NEMS using modified Adomian method. Physica E 2010;43:625–32.
[35] Wazwaz AM. The numerical solution of sixth-order boundary value problems by the modified decomposition method. J Appl Math Comput 2001;118:311–25.
[36] Timoshenko S. Theory of Plates and Shells. New York: McGraw Hill; 1987.
[37] Ke CH, Espiona HD. Nanoelectromechanical systems (NEMS) and modelinb. Handbook of Theoretical and Computional Nanotechnology.American Scientific Publishers; 2006 [Chapter 121].
[38] Legtenberg R, Tilmans HAC, Elders J, Elwenspoek M. Stiction of surface micromachined structures after rinsing and drying: model and investigation of adhesion mechanisms. Sensors Actuators Phys 1994;43:230–8.
[39] Leus V, Elata D. Fringing field effect in electrostatic actuators. Technical Report 2004; ETR-2004-2.
[40] Chen KL, Zhang JW. Comparison of the RF MEMS switches with dielectric layers on the bridge's lower surface and on the transmission line. Sci China Ser 2011;54:396–406.
[41] Rach R. A convenient computational form for the Adomian polynomials. J Math Anal Appl 1984;102:415–9.
[42] Adomian G. Nonlinear Stochastic Operator Equations. New York: Academic press; 1986.
[43] Aly EH, Ebaid A, Rach R. Advances in the Adomian decomposition method for solving two-point nonlinear boundary value problems with Neumann boundary conditions. Appl Math Comput 2012;63:1056–65.
[44] Duan JS, Chaolu T, Rach R. Solutions of the initial value problem for nonlinear fractional ordinary differential equations by the Rach–Adomian–Meyers modified decomposition method. Appl Math Comput 2012;218:8370–92.
[45] Duan JS, Rach R. New higher-order numerical one-step methods based on the Adomian and the modified decomposition methods. Appl Math Comput 2012;218:2810–28.
[46] Duan JS, Rach R. Higher-order numeric Wazwaz–El–Sayed modified Adomian decomposition algorithms. Appl Math Comput 2012;63:1557–68.
[47] Rach R, Duan JS. Near-field and far-field approximations by the Adomian and asymptotic decomposition methods. Appl Math Comput 2011;217:5910–22.
[48] Wazwaz AM. A reliable algorithm for solving boundary value problems for higher-order integro–diferential equations. Appl Math Comput 2001;118:327–42.
[49] Adomian G, Ruch R. Modified Adomian polynomials. Math Comput Model 1996;24:39–46.
[50] Fehlberg E. Low-order classical Runge–Kutta formulas with step size control and their application to some heat transfer problems. NASA Technical Report 31; 1969.
[51] Waters P. Stress analysis and mechanical characterization of thin films for microelectronics and MEMS applications. Doctor of Philosophy, Department of Mechanical Engineering, University of South Florida; 2008.